Effect of Hydration on the Stability of the Collagen-like Triple-Helical Structure of [4(*R*)-Hydroxyprolyl-4(*R*)-hydroxyprolylglycine]$_{10}$‡

Kazuki Kawahara,§ Yoshinori Nishi,§,|| Shota Nakamura,§ Susumu Uchiyama,§,⊥ Yuji Nishiuchi,# Takashi Nakazawa,△ Tadayasu Ohkubo,§ and Yuji Kobayashi*,§,||

Graduate School of Pharmaceutical Sciences, Osaka University, Suita, Osaka 565-0871, Japan, Peptide Institute Inc., Minoh, Osaka 562-8686, Japan, Department of Chemistry, Nara Women's University, Nara 630-8506, Japan, and Osaka University of Pharmaceutical Sciences, Takatsuki, Osaka 569-1094, Japan

Received August 14, 2005; Revised Manuscript Received October 4, 2005

ABSTRACT: X-ray analysis has been carried out on a crystal of the collagen model peptide (Hyp^R-Hyp^R-Gly)$_{10}$ [where Hyp^R is 4(*R*)-hydroxyproline] with 1.5 Å resolution. The triple-helical structure of (Hyp^R-Hyp^R-Gly)$_{10}$ has the same helical parameters and Rich and Crick II hydrogen bond patterns as those of other collagen model peptides. However, our full-length crystal structure revealed that almost all consecutive Hyp^R residues take the up−up pucker in contrast to putative down−up puckering propensities of other collagen model peptides. The unique feature of thermodynamic parameters associated with the conformational transition of this peptide from triple helix to single coil is that both enthalpy and entropy changes of the transition are much smaller than those of other model peptides such as (Pro-Pro-Gly)$_{10}$ and (Pro-Hyp^R-Gly)$_{10}$. To corroborate the precise structural information including main- and side-chain dihedral angles and intra- and interwater bridge networks, we estimated the degrees of hydration by comparing molecular volumes observed experimentally in solution to those calculated ones from the crystal structure. The results showed that the degree of hydration of (Hyp^R-Hyp^R-Gly)$_{10}$ is comparable to that of (Pro-Hyp^R-Gly)$_{10}$ in the triple-helical state, but the former was more highly hydrated than (Pro-Hyp^R-Gly)$_{10}$ in the single-coil state. Because hydration reduces the enthalpy due to the formation of a hydrogen bond with a water molecule and diminishes the entropy due to the restriction of water molecules surrounding a peptide molecule, we concluded that the high thermal stability of (Hyp^R-Hyp^R-Gly)$_{10}$ is able to be described by its high hydration in the single-coil state.

Collagen is the main structural component of skin, bone, and tendon (*1*). One of the main structural features of the collagen molecule is the triple helix, consisting of three polyproline II-like left-handed helices which form a right-handed superhelical structure; these were initially revealed from fiber diffraction studies of X-ray analysis (*2*, *3*). Each polypeptide chain of collagen consists of approximately 300 units of the X-Y-Gly triplet, where X is often proline (Pro) and Y is often Pro or 4(*R*)-hydroxyproline (Hyp^R) (*1*). We first synthesized a series of polytripeptides (X-Y-Gly)$_n$ with a defined number of *n* as collagen mimics and demonstrated that (Pro-Pro-Gly)$_{10}$ takes a triple-helical structure at lower temperature and shows the thermal transition to a single random coil (*4*, *5*). Since then, this peptide has been regarded as the standard for the studies of thermal stability of the collagen-like triple helix. We also showed that (Pro-Hyp^R-Gly)$_{10}$ forms a triple-helical structure which has higher thermal stability with a transition temperature of about 60 °C, which is 30 °C higher than that of (Pro-Pro-Gly)$_{10}$ (*6*−*8*). This suggests that the Hyp^R residue increases the stability of the triple-helical structure. The subsequent high-resolution X-ray analysis of the (Pro-Hyp^R-Gly)$_4$-Pro-Hyp^R-Ala-(Pro-Hyp^R-Gly)$_5$ analogue, which we refer to as Gly → Ala hereafter, has provided the first experimental proof for the existence of water bridges (*9*, *10*). This is consistent with the generally accepted hypothesis that hydrogen bonds involving hydroxyl groups of Hyp^R should act to stabilize the collagen triple helix. This hypothesis was questioned when (Pro-fPro^R-Gly)$_{10}$, containing 4(*R*)-fluoroproline (fPro^R) with a low ability to form a hydrogen bond, was found to fold into a triple helix with extremely high thermal stability (*11*, *12*). However, our recent thermodynamic analyses supported the significance of hydrogen bonds in the thermal stability of the triple-helical structure for Hyp-containing model peptides (*13*). There remains a further problem concerning the apparently contradictory effect of the Hyp residue on the stability of the triple-helical structure with respect to its stereochemistry and sequence position. This includes intriguing phenomena that neither (Hyp^R-Pro-Gly)$_{10}$ nor model peptides containing 4(*S*)-hydroxyproline (Hyp^S), (Pro-Hyp^S-Gly)$_{10}$ and (Hyp^S-Pro-Gly)$_{10}$, form a triple-helical structure even at 4 °C (*14*, *15*).

‡ The coordinates of the X-ray structure have been deposited in the Protein Data Bank as entry 1WZB.

* To whom correspondence should be addressed. Telephone: +81-6-6879-8220. Fax: +81-6-6879-8224. E-mail: yujik@protein.osaka-u.ac.jp.

§ Osaka University.

|| Osaka University of Pharmaceutical Sciences.

⊥ Present address: Department of Biotechnology, Graduate School of Engineering, Osaka University.

Peptide Institute Inc.

△ Nara Women's University.

10.1021/bi051619m CCC: $30.25
Published on Web 11/10/2005

To explain these substitution effects, Zagari and co-workers have elucidated an empirical rule, the so-called propensity-based rule, of the pyrrolidine ring pucker for the stability of collagen triple helix using the X-ray analytical data on various collagen model peptides (*16*, *17*); the puckering should be down at the X position and up at the Y position in the triple helix of collagen model peptides (X-Y-Gly)$_n$. According to the computational investigations allowing for the electron-withdrawing effects of the hydroxyl group and fluorine atom, it is confirmed that Hyp^R and fPro^R prefer the up form and that Hyp^S and 4(*S*)-fluoroproline (fPro^S) prefer the down form, whereas Pro can take both forms (*18*−*23*). It is thus reasonable to presume that a stable triple helix could arise when the X position is occupied with Hyp^S and the Y position with Hyp^R. This could explain the substitution effect in the cases of (Hyp^R-Pro-Gly)$_{10}$ and (Pro-Hyp^S-Gly)$_{10}$ but not the fact that (Hyp^S-Pro-Gly)$_{10}$ does not form a stable triple helix, whereas Hyp^S at the X position could be presumed to enhance the stability of the triple helix due to its propensity to the down pucker.

To address these issues, (Hyp^R-Hyp^R-Gly)$_{10}$ could provide a versatile example concerning the effect of an extra Hyp^R residue on the tendencies of (Hyp^R-Pro-Gly)$_{10}$ and (Pro-Hyp^R-Gly)$_{10}$ to stabilize and destabilize the triple helix, respectively. In fact, (Hyp^R-Hyp^R-Gly)$_{10}$ did form a thermally stable triple helix (*24*−*26*), despite its predicted instability according to a propensity-based rule that requires the pyrrolidine ring pucker be down at the X position and up at the Y position (*16*). In the previous thermodynamic studies, we suggested that the stability of this peptide could not be explained by resorting to the empirical rule of ring pucker but be analyzed individually by careful thermodynamic investigations in combination with precise crystallographic data (*26*). A recent report by Bächinger and co-workers has clearly shown that the ring pucker of the consecutive Hyp^R residues is up−up in the crystal structure of (Gly-Hyp^R-Hyp^R)$_9$ (*27*), thus illuminating the need of an alternative route leading to the comprehensive understanding of the stability of the collagen triple helix.

Here we report the successful determination of the full-length crystal structure of (Hyp^R-Hyp^R-Gly)$_{10}$ at 1.5 Å resolution. The results confirmed the reported structure of (Gly-Hyp^R-Hyp^R)$_9$ (*27*) at large, including important features that almost all of the Hyp^R-Hyp^R unit in the (Hyp^R-Hyp^R-Gly)$_{10}$ crystal structure has up−up conformation and that the triple-helical structure of (Hyp^R-Hyp^R-Gly)$_{10}$ has 7/2 helical symmetry. However, the results from X-ray analysis alone are not sufficient to explain its characteristic thermodynamic properties such as high transition temperature and lower enthalpy and entropy changes of the transition than those of (Pro-Hyp^R-Gly)$_{10}$ (*26*). To correlate the crystallographic structure and thermodynamic parameters, we paid particular attention to the hydration structure of the triple helix, because we recently suggested that the difference between the molecular volumes observed in solution and intrinsic ones calculated from the crystal structure concerning collagen model peptides indicates the degree of hydration which influences the enthalpy and entropy changes of the transition (*13*). In this context, we determined the partial molar volumes of (Hyp^R-Hyp^R-Gly)$_{10}$ in the both triple-helix and single-coil states. Together with structural results, the stabilizing mechanism of (Hyp^R-Hyp^R-Gly)$_{10}$ was elucidated.

EXPERIMENTAL PROCEDURES

Crystallization. (Hyp^R-Hyp^R-Gly)$_{10}$ was synthesized and purified as reported previously (*26*). Initial crystals were obtained by the vapor diffusion method using Crystal Screen kits I and II (Hampton Research Co., Ltd.). The orthorhombic crystals of (Hyp^R-Hyp^R-Gly)$_{10}$ were grown to appropriate size for X-ray diffraction measurement in 1 week at 277 K when poly(ethylene glycol) 4000 was used as the precipitating agent. Refinement of this condition was performed by varying the pH and mixing cryoprotectants. The best crystals for crystallographic analysis were obtained from the drop that consisted of 2 μL of peptide solution (23 mg mL^{-1}) and 2 μL of reservoir solution containing 20% (w/v) poly(ethylene glycol) 4000 and 20% (w/v) 2-propanol in 0.2 M Tris buffer at pH 8.3. The crystals were cubic with typical dimensions of approximately 0.5 mm × 0.4 mm × 0.3 mm.

Data Collection. Diffraction data of the crystal mounted on a cryoloop (0.3−0.4 mm; Hampton Research Co.) were collected at 100 K on an *R*-axis IV^{++} imaging plate detector using Cu Kα radiation equipped with a Rigaku MicroMax-007 and confocal mirror optics. Data processing was performed using the Crystal Clear version 1.3.5 software (*28*). Data up to a maximum resolution of 1.5 Å were collected. The whole diffraction pattern was characterized by two types of reflections, subcell (with short *c* axes, $c' = 22.41$ Å) and unit cell (with long *c* axes, $c = 90.96$ Å). The spots from the unit cell were indexed in the $P2_1$ space group with parameters $a = 18.41$ Å, $b = 19.11$ Å, and $c = 90.96$ Å. For one molecule of molecular mass 2.8 kDa per asymmetric unit ($Z = 2$), the Matthews coefficient is 1.9 Å^3 Da^{-1} and the solvent content is 33.6% (*29*).

Phase Determination and Refinements. Phase determination was performed by using ACORN-MR (*30*) with the whole structure of the (Pro-Pro-Gly)$_{10}$ (PDB entry 1K6F) as a search model (*31*). The best score of the correlation coefficient from ACORN-MR was 0.517. The phases from ACORN were input into the warpNtrace mode of ARP/wARP (*32*). The main-chain trace consisting of 69 out of 90 residues in three poly-Gly chains was built automatically. Then, the missing parts were manually rebuilt with the molecular graphics program Xfit implemented in XtalView (*33*). In the next step, the poly-Gly chains were replaced manually by Pro or Hyp^R using XtalView. Maximum-likelihood refinement of the resulting model and water picking were carried out by REFMAC5 (*34*). The final model consisted of 767 non-H protein atoms and 177 water molecules; the resulting R_{factor} and R_{free} are 0.172 and 0.200, respectively. Data collection and refinement statistics are reported in Table 1. The coordinates of the (Hyp^R-Hyp^R-Gly)$_{10}$ crystal structure have been deposited in the RCSB Protein Data Bank (entry 1WZB).

CD Measurements. Measurements of CD[1] spectra were carried out on a JASCO J-720W spectropolarimeter with the airtight pressure-proof cell compartment. The details of the airtight pressure-proof cell compartment are described in refs *35* and *36*. The temperature-dependent CD ellipticity, in the range of 210−260 nm, was obtained with a cell of 1 mm path length by averaging 16 scans. The spectra were recorded

[1] Abbreviations: ASA, accessible surface area; CD, circular dichroism; DSC, differential scanning calorimetry; PDB, Protein Data Bank.

Table 1: Crystallographic Parameters and Refinement Statistics[a]

space group	$P2_1$
unit cell	
a, *b*, *c*/Å	18.41, 19.11, 90.96
α, *β*, *γ*/deg	90, 94.26, 90
resolution range/Å	10.0−1.5 (1.538−1.500)
no. of reflections	9772
completeness/%	98.22 (98.60)
no. of atoms	767
no. of water molecules	177
rmsd from ideal values	
bond distances/Å	0.005
bond angles/deg	2.8
overall *B* factor/Å^2	8.31
R_{factor} (including test reflections)	0.172
R_{work}	0.170 (0.175)
R_{free}	0.200 (0.202)

[a] Values in parentheses are for the highest resolution shell.

from 40 to 160 °C with temperature intervals of 10 °C. The heating rate was 0.1 K min^{-1}, which is slow enough to attain the equilibrium condition as shown in our previous study (*7*, *13*). (Hyp^R-Hyp^R-Gly)$_{10}$ was dissolved in 100 mM AcOH at a concentration of 0.045 mM.

Partial Specific Volume Determination. The partial specific volume of a solute ($\bar{v}$) is obtained from the concentration dependence of the density of the solution using the equation

$$\left(\frac{\partial\rho}{\partial c}\right)_{m,p} = 1 - \bar{v}\rho_0 \qquad (1)$$

where ρ and ρ_0 are the densities of the solution and the solvent, respectively (*37*). The density of the solution of (Hyp^R-Hyp^R-Gly)$_{10}$ was measured using a vibrational density meter, Anton Paar DMA 5000. The density of the solution of the peptide was measured at 10 and 80 °C with an exception of (Pro-Pro-Gly)$_{10}$ at 10 and 70 °C (within ±0.01 °C) and collected by taking the average of three measurements (within $\pm 5 \times 10^{-6}$ g cm^{-3}). The concentration of a peptide in solution was determined on the basis of the amino acid analysis (see the Supporting Information).

Calculations of the Intrinsic Molecular Volume and the Accessible Surface Area (ASA). The atomic coordinates of (Hyp^R-Hyp^R-Gly)$_{10}$ in the single-coil state were obtained by energy minimization using X-PLOR (*38*) as already reported in our last paper (*13*). The intrinsic volumes of (Hyp^R-Hyp^R-Gly)$_{10}$ in the triple-helix and single-coil states ($V_{int,t}$ and $V_{int,s}$, respectively) were evaluated using MSRoll (*39*). Total ASAs of the model peptide (Hyp^R-Hyp^R-Gly)$_{10}$ in the triple-helix and single-coil states ($ASA_{total,t}$ and $ASA_{total,s}$, respectively), which consist of polar (amide N, carbonyl O, and hydroxyl O) and nonpolar (aliphatic C and carbonyl C) components ($ASA_{pol,t}$, $ASA_{pol,s}$, $ASA_{npol,t}$, and $ASA_{npol,s}$, respectively), were calculated using MSRoll (*39*), with the probe radius of water (equal to 1.4 Å). These values are expressed per tripeptide Hyp^R-Hyp^R-Gly unit.

RESULTS

Overall Structure. The full-length structure of (Hyp^R-Hyp^R-Gly)$_{10}$ was determined and refined at 1.5 Å resolution. In an asymmetric unit, the triple helix of (Hyp^R-Hyp^R-Gly)$_{10}$ had a rodlike structure about 90 Å long with a diameter of 10 Å, and each strand was staggered by one residue (Figure 1, A, B, and C denote three chains distinguished for convenience). All of the residues were well defined on the electron density map with the exception of the N-terminal 4(*R*)-hydroxyproline (Hyp^R 1, chain C) and the C-terminal glycine (Gly 30, chain B). In the triple helix, the Rich and Crick II hydrogen bonds between the N−H groups of glycine and the C═O groups of Hyp^R residues at the X positions of the adjacent chains were observed with the averaged length of 2.89 Å, which is within the range commonly found in other collagen model peptides as shown in Table 2. The averaged values of the unit height and unit twist of (Hyp^R-Hyp^R-Gly)$_{10}$ were 8.4 Å and 51.4°, respectively, as shown in Table 3. These values are close to those of other collagen model peptides with 7/2 symmetry (*40*−*45*).

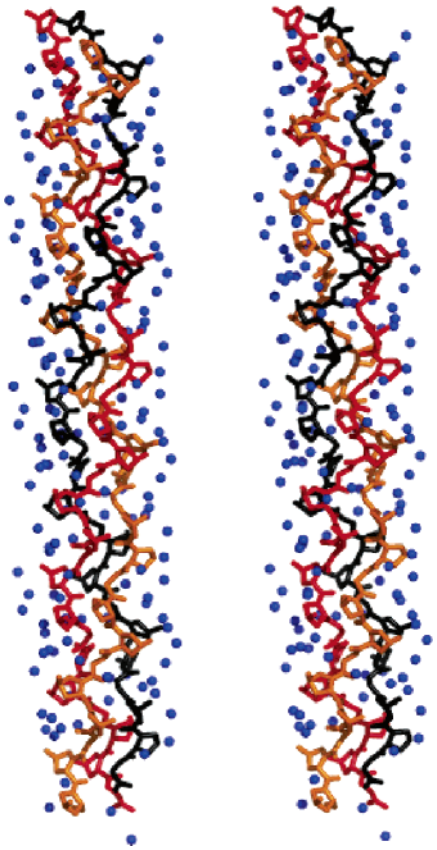

FIGURE 1: Stereoview of the crystal structure of (Hyp^R-Hyp^R-Gly)$_{10}$ in the asymmetric unit (chain A, red; chain B, orange; chain C, black). Water molecules are also shown and colored in blue. This figure was generated by PyMOL (*46*).

Table 2: Rich and Crick II Interchain Hydrogen Bond Parameters of (Hyp^R-Hyp^R-Gly)$_{10}$ along with Those of Gly → Ala and (Pro-Pro-Gly)$_{10}$

	this work	Gly → Ala[a]	(Pro-Pro-Gly)$_{10}$[b]
distance/Å	2.89 (0.05)[c]	2.94 (0.08)	2.97 (0.06)
angle/deg	167 (2)	163 (5)	167 (2)

[a] Reference *9*. [b] Reference *31*. [c] Standard deviations are given in parentheses.

Table 3: Helical Parameters of (Hyp^R-Hyp^R-Gly)$_{10}$ along with Those of Gly → Ala and (Pro-Pro-Gly)$_{10}$

	this work	Gly → Ala	(Pro-Pro-Gly)$_{10}$
helical height/Å	8.4	8.4	8.5
unit twist/deg	51.4	51.4	51.5

Table 4: Averaged Values of Backbone Dihedral Angles ϕ, ψ, and ω of (Hyp^R-Hyp^R-Gly)$_{10}$ along with Those of Gly → Ala and (Pro-Pro-Gly)$_{10}$[a]

	this work	Gly → Ala	(Pro-Pro-Gly)$_{10}$
ϕ X position/deg	−64.9 (4.1)	−72.6 (7.6)	−74.5 (2.9)
ψ X position/deg	155.3 (4.2)	163.8 (8.8)	164.3 (4.1)
ω X position/deg	170.2 (2.7)	179.9 (1.8)	176.0 (2.5)
ϕ Y position/deg	−55.1 (3.1)	−59.6 (7.3)	−60.1 (3.6)
ψ Y position/deg	148.2 (1.8)	149.8 (8.8)	152.4 (2.6)
ω Y position/deg	177.6 (2.2)	178.5 (1.5)	175.4 (3.4)
ϕ Gly/deg	−69.1 (3.4)	−71.9 (9.6)	−71.7 (3.7)
ψ Gly/deg	172.4 (3.3)	174.1 (11.9)	175.9 (3.1)
ω Gly/deg	177.1 (1.6)	177.3 (3.1)	179.7 (2.0)

[a] Standard deviations are given in parentheses. Because the averaged temperature factor of the terminal residues (chain A, 1, 2, 29, 30; chain B, 1, 2, 29, 30; chain C, 1, 2, 29, 30) is significantly higher than that of all the other residues of (Hyp^R-Hyp^R-Gly)$_{10}$, these terminal residues were omitted from the calculation of average.

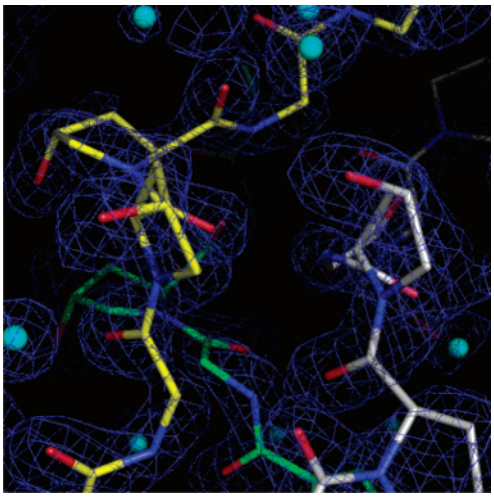

FIGURE 2: Electron density maps (omit map) of the crystal structure of (Hyp^R-Hyp^R-Gly)$_{10}$.

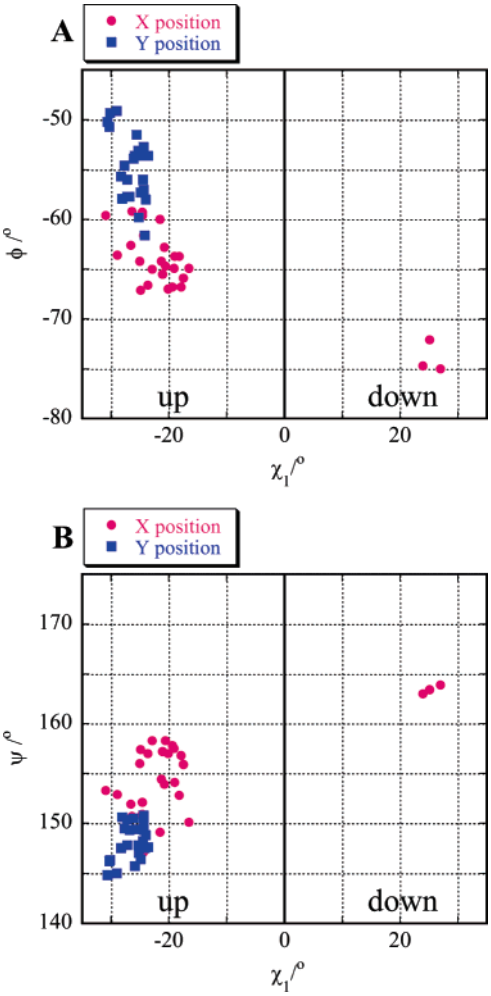

FIGURE 3: Plots of ϕ versus χ_1 (A) and ψ versus χ_1 (B) for Hyp^R rings in the X (red circles) and Y (blue squares) positions of (Hyp^R-Hyp^R-Gly)$_{10}$.

The main-chain dihedral angles ϕ, ψ, and ω were determined and averaged over a molecule in an asymmetric unit as listed in Table 4.

Side-Chain Conformation and Pyrrolidine Ring Puckering. In the crystal structure of (Hyp^R-Hyp^R-Gly)$_{10}$, we obtained electron density maps that clearly identify pyrrolidine ring puckering in each Hyp^R residue (Figure 2). In Figure 3, the relationships between dihedral angles ϕ and χ_1 and those between ψ and χ_1 of (Hyp^R-Hyp^R-Gly)$_{10}$ were plotted. Because of the conformational disorder resulting from the manner of chain alignment where each strand was not in register, the averaged temperature factor of the terminal residues is significantly higher than that of all the other residues of (Hyp^R-Hyp^R-Gly)$_{10}$ as reported in other collagen model peptides, (Pro-Pro-Gly)$_{10}$ and Gly → Ala (*10*, *31*). Therefore, nine terminal Hyp^R residues (chain A, 1, 2, 29; chain B, 1, 2, 29; chain C, 1, 2, 29) were omitted from the plots. Figure 3 showed that 48 out of 51 Hyp^R residues in the (Hyp^R-Hyp^R-Gly)$_{10}$ model adopt up (negative χ_1) pucker, whereas the remaining three Hyp^R residues adopt down (positive χ_1) pucker. The conformations of Hyp^R residues which take up pucker are separated into two groups with different average angles of ϕ and ψ depending on their positions such that Hyp^R at the X position takes −64.9° and 155.3° and Hyp^R at the Y position takes −55.1° and 148.2°. Note that there are distinct differences between conformations of Hyp^R residues depending on their positions despite the fact that the up pucker is found in common. The exceptional three residues which take down pucker are A10, B16, and C25, and all are located at the X position.

Molecular Packing and Direct Interactions among Triple Helices. Similar to crystals of (Pro-Pro-Gly)$_{10}$ and Gly → Ala model peptides, the triple helices of (Hyp^R-Hyp^R-Gly)$_{10}$ are antiparallel to each other and packed axially in the manner of head to tail, probably enabling the charge−charge interaction between N- and C-terminal residues (*9*, *31*). The packing of (Hyp^R-Hyp^R-Gly)$_{10}$ is pseudotetragonal (Figure 4a). As schematically illustrated in Figure 4a, one triple helix is directly connected by six hydrogen bonds with the averaged distance of 2.76 Å between the hydroxyl groups of Hyp^R residues at the X position belonging to two adjacent helices. At each contacting surface between any of two triple helices, there arise three pairs of Hyp^R residues at A10−B22, B16−A16, and C25−C10. As shown in Figure 4b, these hydrogen bonds are stacked respectively in a line parallel with the major axis of each triple helix. It is worth noting that A10, B16, and C25 involved in the in-line hydrogen bond formation correspond to the three residues themselves which take exceptionally down pucker. The counterparts of the hydrogen bond formation in the neighboring triple helix are hydroxyl groups of Hyp^R residues with up pucker. Triple helices in the crystal of (Hyp^R-Hyp^R-Gly)$_{10}$

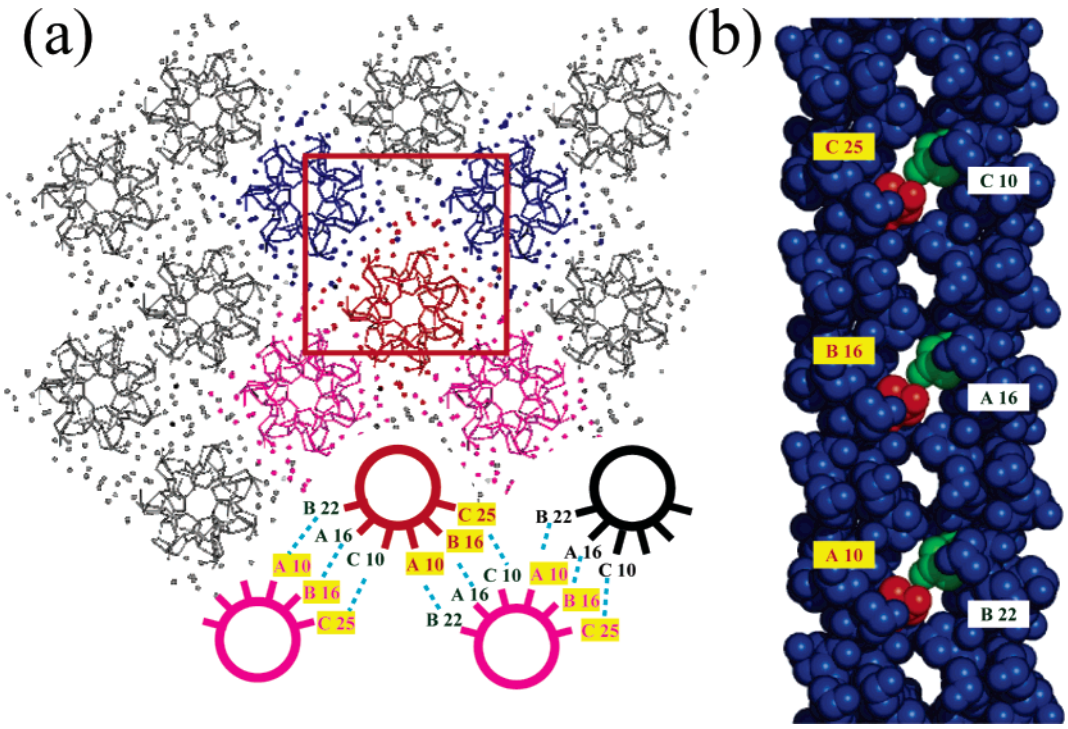

FIGURE 4: (a) Lateral packing of the triple helices of $(Hyp^R\text{-}Hyp^R\text{-}Gly)_{10}$ and illustration of direct interactions among triple helices. The reference molecule (red) forms direct hydrogen bonds with two out of four neighboring helices (purple). Two other neighbors (blue) interact with the reference molecule through a few water molecules. Hyp^R residues marked by a yellow background adopt down pucker. Dotted lines (sky blue) designate the hydrogen bonds. (b) Direct hydrogen bond interactions of two adjacent helices. Among the Hyp^R residues involving direct hydrogen bond interactions of two adjacent helices, the ones with up pucker are in green and the ones with down pucker are in red.

interact with each other through these hydrogen bonds in a zigzag form at about 90°.

Hydration. An asymmetric unit of the crystal of the triple helix of $(Hyp^R\text{-}Hyp^R\text{-}Gly)_{10}$ contains 177 water molecules. Water molecules were considered to be involved in hydrogen bonds within a 3.25 Å cutoff distance from the polar groups or other water molecules. Almost all water molecules observed in the crystal are not isolated so as to be hydrogen-bonded to the peptide chains to form a layer of framework coating its surface or bonded to at least one neighboring water molecule. They are involved in water bridges stabilizing the peptide conformation as in the cases of other collagen model peptides (*9*, *10*, *44*, *45*). Four types of water bridges which have been found by Berman and co-workers in the Gly → Ala peptide are classified to α [intrachain bridge between the Hyp^R(Y) C═O group and the Gly C═O group], *β* [interchain bridge between the Hyp^R(Y) C═O group and the Gly C═O group], *γ* [intrachain bridge between the Hyp^R-(Y) OH group and the Gly C═O group], and *δ* [interchain bridge between the Hyp^R(Y) OH group and the Hyp^R(Y) C═O group] (*10*). In $(Hyp^R\text{-}Hyp^R\text{-}Gly)_{10}$, the following three types of water bridges were newly observed as displayed in Figure 5. We denote these as *κ* [interchain bridge between the Hyp^R(X) OH group and the Gly C═O group], *λ* [intrachain bridge between the Hyp^R(X) OH group and the Hyp^R(Y) OH group], and *μ* [interchain bridge between the Hyp^R(X) OH group and the Hyp^R(Y) OH group]. Various numbers of water molecules are involved in each water bridge. For example, two or three water molecules are utilized in interchain *κ* bridges which are named *κ*2 bridge and *κ*3 bridge, respectively. (The same shall apply hereafter.) One to three water molecules are involved in intrachain *λ* bridges and two or three in interchain *μ* bridges. The frequencies of occurrence of each type of water bridge in the crystal of $(Hyp^R\text{-}Hyp^R\text{-}Gly)_{10}$ are summarized by the number of cases in Table 5.

CD Measurements. The CD spectra of $(Hyp^R\text{-}Hyp^R\text{-}Gly)_{10}$ at 40−160 °C are shown in Figure 6A. The melting profile of $(Hyp^R\text{-}Hyp^R\text{-}Gly)_{10}$ is shown in Figure 6B. At 40 °C, the spectrum has a positive peak around 225 nm, which is the characteristic of a collagen triple helix. As temperature increases, the intensity of the positive peak decreases. At high temperature, it is indicated that the model peptide does not take any ordered structure because the spectrum has a negative absorption at 225 nm.

Observed and Calculated Molar Volume. It was hard to carry out the density measurement of peptide solution at higher than 80 °C because of the instrumental limit of the densitometry. However, the melting profile of $(Hyp^R\text{-}Hyp^R\text{-}Gly)_{10}$ obtained by CD measurement in Figure 6B showed that the conformational transition of $(Hyp^R\text{-}Hyp^R\text{-}Gly)_{10}$ has almost completed (less than 1%) at this temperature. Thus, we could assume that $(Hyp^R\text{-}Hyp^R\text{-}Gly)_{10}$ exists dominantly in the single-coil state at 80 °C. The densities of $(Hyp^R\text{-}Hyp^R\text{-}Gly)_{10}$ measured at that temperature showed a linear dependency on the concentration as shown in Figure S1 in the Supporting Information. According to eq 1, the slope of the line provided the partial specific volume of $(Hyp^R\text{-}Hyp^R\text{-}Gly)_{10}$ in the single-coil state to be 0.6204 $cm^3\ g^{-1}$. The value of $(Hyp^R\text{-}Hyp^R\text{-}Gly)_{10}$ in the triple-helix state was obtained to be 0.6024 $cm^3\ g^{-1}$ as previously reported (*26*). These values are listed in Table 6 with calculated values of intrinsic volume and ASA.

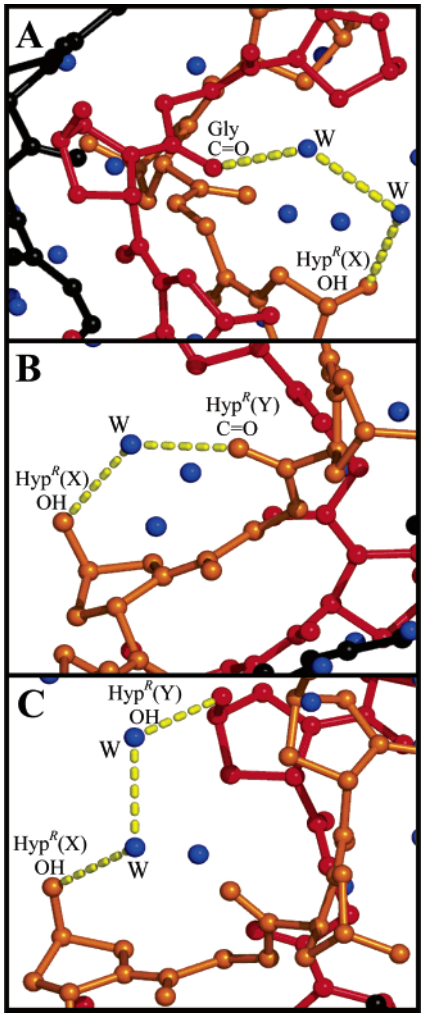

FIGURE 5: An example of various types of water bridges. (A) Interchain κ2 bridge between the Hyp^R(X) OH group and the Gly C═O group. (B) Intrachain λ1 bridge between the Hyp^R(X) OH group and the Hyp^R(Y) C═O group. (C) Interchain μ2 bridge between the Hyp^R(X) OH group and the Hyp^R(Y) OH group. Dotted lines (yellow) designate the hydrogen bonds. Water molecules (blue) which are involved in the water bridge are labeled by W.

Table 5: Number of Water Bridges in the Crystal Structure of (Hyp^R-Hyp^R-Gly)$_{10}$

bridge	connectivity	type	no. of cases
α bridge	intrachain	α1	2
		α2	8
		α3	10
β bridge	interchain	β3	4
γ bridge	intrachain	γ2	25
δ bridge	interchain	δ2	19
		δ3	1
κ bridge	interchain	κ2	14
		κ3	5
λ bridge	intrachain	λ1	15
		λ2	9
		λ3	2
μ bridge	interchain	μ2	15
		μ3	5

It is widely accepted that the observed partial molar volume ($\bar{V}_{obs}$) is the sum of intrinsic volume (V_{int}), hydration volume (V_{hyd}), and thermal motion volume (V_{therm}), which is proportional to total ASA. Here, presuming the thermal motion volume of a peptide in the triple-helix state ($V_{therm,t}$) equals to 0.040 ASA$_{total,t}$ as reported in ref *13*, we obtained the $V_{therm,t}$ value of 22.8 cm^3 mol^{-1} for (Hyp^R-Hyp^R-Gly)$_{10}$. Using this value and $\bar{V}_{obs,t}$ with $V_{int,t}$ values of (Hyp^R-Hyp^R-Gly)$_{10}$ listed in Table 6, $V_{hyd,t}$ for (Hyp^R-Hyp^R-Gly)$_{10}$ was deduced to be −19.0 cm^3 mol^{-1}.

We estimated the degree of hydration of the single-coil state in the same way as we did for the triple helix. The details of calculation are described in the Supporting Information. The hydration volumes of a peptide in the single-coil state ($V_{hyd,s}$) for (Pro-Pro-Gly)$_{10}$, (Pro-Hyp^R-Gly)$_{10}$, and (Hyp^R-Hyp^R-Gly)$_{10}$ were estimated to be −2.6, −4.0, and −7.3 cm^3 mol^{-1}, respectively. In Table 6, related data in our previous paper for (Pro-Pro-Gly)$_{10}$ and (Pro-Hyp^R-Gly)$_{10}$ are also listed for reference (*13*).

DISCUSSION

In the previous report, we suggested that the stability of the collagen-like triple helix is largely influenced by the interaction with the solvent molecules (*13*). The present X-ray analysis could provide the previous thermodynamic study with the complementary information by giving the precise structural data of not only the peptide but also the solvent molecules. The most distinguished structural feature of (Hyp^R-Hyp^R-Gly)$_{10}$ in the crystal is that almost all consecutive Hyp^R residues take up−up pucker in contrast to their putative down (X position)−up (Y position) puckering propensities, although the overall structure of (Hyp^R-Hyp^R-Gly)$_{10}$ appears to be similar to those of the other polytripeptides with 7/2 helix symmetry. If the high thermal stability of (Hyp^R-Hyp^R-Gly)$_{10}$ could be associated with such a unique up−up pucker, a new stabilization mechanism should be elaborated on the basis of the detailed comparison of structural features between (Hyp^R-Hyp^R-Gly)$_{10}$ and the other collagen model peptides. In this context, we first compared (Hyp^R-Hyp^R-Gly)$_{10}$ with those of other collagen-like model peptides such as Gly → Ala and (Pro-Pro-Gly)$_{10}$ in (1) backbone dihedral angles, ϕ, ψ, and ω, and (2) the Rich and Crick II hydrogen bond parameters.

Comparison of Structural Parameters of (Hyp^R-Hyp^R-Gly)$_{10}$ with Those of the Other Collagen Model Peptides. It is obvious that the ω values of all positions in these model peptides, (Hyp^R-Hyp^R-Gly)$_{10}$, Gly → Ala, and (Pro-Pro-Gly)$_{10}$, are almost the same, as listed in Table 4. However, when the variations of dihedral angles (ϕ, ψ) at each position were displayed in the ϕ−ψ plane, as shown in Figure 7A, there are appreciable deviations in the distributions of the values of (ϕ, ψ) at the X position among the three peptides. The center of distribution of values of (Hyp^R-Hyp^R-Gly)$_{10}$, except for three values, deviates from those of Gly → Ala and (Pro-Pro-Gly)$_{10}$ by shifting toward down and right in the ϕ−ψ plane. On the other hand, the deviations of those values at the Y position are rather small in Figure 7B, and there is no deviation for those at the Gly position in Figure 7C. The results of a statistical survey on the pyrrolidine rings of proline residues in protein structures reveal that the averaged ϕ value is about −60° in Pro with up pucker and about −70° in Pro with down pucker (*17*). The fact that the ϕ values at the X position of (Hyp^R-Hyp^R-Gly)$_{10}$ distributed around −60° rather than −70° whereas those of Gly → Ala and (Pro-Pro-Gly)$_{10}$ are around −70° reinforces that (Hyp^R-Hyp^R-Gly)$_{10}$ has up−up conformation.

As for the three exceptional Hyp^R residues in Figure 7A, they correspond to the above-mentioned residues involved

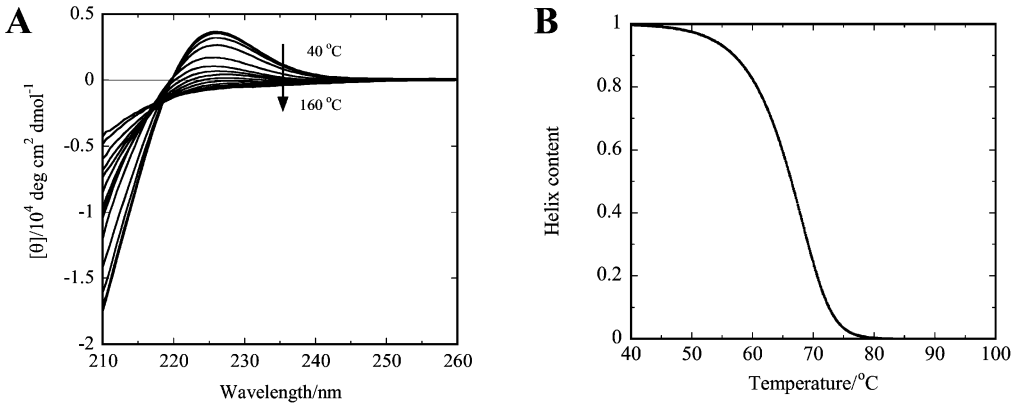

FIGURE 6: (A) Temperature dependencies of CD spectra of $(Hyp^R\text{-}Hyp^R\text{-}Gly)_{10}$. (B) Melting profile of $(Hyp^R\text{-}Hyp^R\text{-}Gly)_{10}$ obtained by CD measurement.

Table 6: Observed Partial Specific ($\bar{v}_{obs}$), Observed Partial Molar ($\bar{V}_{obs}$), and Intrinsic Molecular (V_{int}) Volumes and the Difference between $\bar{V}_{obs}$ and V_{int} ($\bar{V}_{obs} - V_{int}$), Hydration Volume (V_{hyd}), and ASAs of $(Hyp^R\text{-}Hyp^R\text{-}Gly)_{10}$ along with Those of $(Pro\text{-}Pro\text{-}Gly)_{10}$ and $(Pro\text{-}Hyp^R\text{-}Gly)_{10}$ in the Single-Coil State (s) and Triple-Helix State (t)

peptide	state	$\bar{v}_{obs}$/cm^3 g^{-1}	$\bar{V}_{obs}$/cm^3 mol^{-1} [d]	V_{int}/ cm^3 mol^{-1} [d]	$\bar{V}_{obs} - V_{int}$/ cm^3 mol^{-1} [d]	V_{hyd}/ cm^3 mol^{-1} [d]	ASA_{total}/ Å^2 [d]	ASA_{pol}/ Å^2 [d]	ASA_{npol}/ Å^2 [d]
$(Hyp^R\text{-}Hyp^R\text{-}Gly)_{10}$	s[a]	0.6204 (0.00398)[g]	176.9 (1.13)	150.0	26.9 (1.1)	−7.3 (1.1)	1033.5	489.7	543.8
	t[c]	0.6024[e] (0.00574)	171.7 (1.64)	169.0	2.7 (1.6)	−19.0 (1.6)	569.9	285.8	284.1
$(Pro\text{-}Pro\text{-}Gly)_{10}$	s[b]	0.7008 (0.00126)	177.4 (0.319)	147.0	30.4 (0.32)	−2.6 (0.32)	997.7	237.7	760.0
	t[c]	0.6692[f] (0.00055)	169.4[f] (0.139)	157.4[f]	12.0[f] (0.14)	−9.6[f] (0.14)	539.8[f]	79.6[f]	460.2[f]
$(Pro\text{-}Hyp^R\text{-}Gly)_{10}$	s[a]	0.6624 (0.00477)	178.2 (1.28)	148.5	29.7 (1.3)	−4.0 (1.3)	1015.6	363.7	651.9
	t[c]	0.6120[f] (0.00287)	164.7[f] (0.772)	161.5[f]	3.2[f] (0.77)	−18.6[f] (0.77)	543.7[f]	154.6[f]	389.1[f]

[a] Observed at 80 °C. [b] Observed at 70 °C. [c] Observed at 10 °C. [d] Expressed per tripeptide unit. [e] From ref *26*. [f] From ref *13*. [g] Standard errors are given in parentheses.

in the interhelix hydrogen bonds at the X position. Because their average values (ϕ, ψ) correspond to the values for down pucker as those of Pro residues at the X position of Gly → Ala and $(Pro\text{-}Pro\text{-}Gly)_{10}$, it is confirmed that these residues of $(Hyp^R\text{-}Hyp^R\text{-}Gly)_{10}$ exceptionally take down pucker at the X position.

It is quite interesting that, despite this unique conformation, $(Hyp^R\text{-}Hyp^R\text{-}Gly)_{10}$ takes a triple-helical structure sharing the characteristic features of collagen-like structure as helical parameters of the 7/2 model and interstrand Rich and Crick II hydrogen bonds with Gly → Ala and $(Pro\text{-}Pro\text{-}Gly)_{10}$.

As listed in Table 4, the average values of (ϕ, ψ) at the X position were (−64.9°, 155.3°) for $(Hyp^R\text{-}Hyp^R\text{-}Gly)_{10}$ [if omitting the exceptional three residues of down pucker with the average values of (−73.9°, 163.4°), the averages are (−63.7°, 154.4°)], (−72.6°, 163.8°) for Gly → Ala, and (−74.5°, 164.3°) for $(Pro\text{-}Pro\text{-}Gly)_{10}$. Those at the Y position were (−55.1°, 148.2°) for $(Hyp^R\text{-}Hyp^R\text{-}Gly)_{10}$, (−59.6°, 149.8°) for Gly → Ala, and (−60.1°, 152.4°) for $(Pro\text{-}Pro\text{-}Gly)_{10}$. The standard values of (ϕ, ψ) for Hyp^R have been calculated to be (−63.1°, 146.3°) for up pucker and (−70.5°, 167.7°) for down pucker as the minimum energy geometry in a dipeptide analogue of Hyp^R by the quantum mechanical study of Improta et al. (*22*). These values of side-chain dihedral angles χ_1, χ_2, χ_3, and χ_4 of Hyp^R pyrrolidine rings are also given and listed in Table S1 in the Supporting Information.

Even though Hyp^R residues at both of the X and Y positions adopt up pucker and their side-chain dihedral angles χ_1, χ_2, χ_3, and χ_4 were very close to those of the standard values of Hyp^R with up pucker, there is an obvious difference between main-chain dihedral angles of Hyp^R residues at each position and those of standard values of Hyp^R with up pucker.

The standard values of dihedral angles (−63.1°, 146.3°) are very close to the ϕ value of Hyp^R at the X position (−63.7°) and the ψ value of Hyp^R at the Y position (148.2°), respectively. In contrast, the ϕ value of Hyp^R at the Y position (−55.1°) and the ψ value of Hyp^R at the X position (154.1°) in $(Hyp^R\text{-}Hyp^R\text{-}Gly)_{10}$ have deviated from these values.

There is no clear explanation so far for the fact that, while the values of dihedral angles at the Y position are almost the same among these three peptides, those of $(Hyp^R\text{-}Hyp^R\text{-}Gly)_{10}$ at the X position are unique but its ϕ value is very close to the standard value. If we build up a hypothetical structure assuming the dihedral values at the X position of $(Hyp^R\text{-}Hyp^R\text{-}Gly)_{10}$ to be the standard values of Hyp^R, the interstrand Rich and Crick II hydrogen bonds could not exist (see Figure S2 in the Supporting Information).

We now consider that this minor adjustment on the dihedral angles does not impose enough strain to alter the up pucker of Hyp^R residues at the X position, thus preserving the triple-helical structure of $(Hyp^R\text{-}Hyp^R\text{-}Gly)_{10}$. The resulting strain could be compensated at least partly by the hydration involving the hydroxyl group of Hyp^R at the X position of the triple helix as stated below. It is therefore necessary to explain why the unique up−up pucker could provide $(Hyp^R\text{-}Hyp^R\text{-}Gly)_{10}$ with an additional or comparable stability to those of Gly → Ala and $(Pro\text{-}Pro\text{-}Gly)_{10}$, both of which adopt the down−up pucker. Another possible factor to be considered responsible for stabilizing the triple helix is the interaction with water molecules, especially when they are involved in the hydrogen bond network around the triple helix.

While we were preparing this report, Bächinger and coworkers published the crystal structure of $(Gly\text{-}Hyp^R\text{-}Hyp^R)_9$

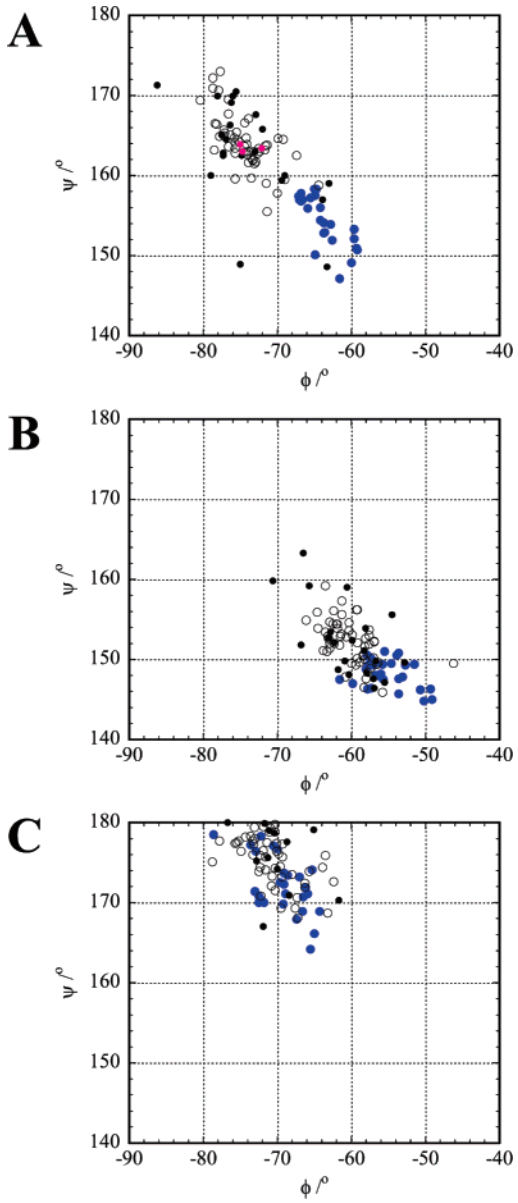

FIGURE 7: Plots of ϕ versus ψ of (Hyp^R-Hyp^R-Gly)$_{10}$ (blue circles), Gly → Ala (black circles), and (Pro-Pro-Gly)$_{10}$ (open circles). (A) Pro or Hyp^R residues at the X position. Three Hyp^R residues with down pucker at the X position of (Hyp^R-Hyp^R-Gly)$_{10}$ are displayed in red circles. (B) Pro or Hyp^R residues at the Y position. (C) Gly residues.

(*27*). Although both crystal structures indeed exhibit 7/2 helical symmetry and have up−up pucker in almost all Hyp^R-Hyp^R units, there are recognizable differences such that the crystal of (Gly-Hyp^R-Hyp^R)$_9$ has a pseudohexagonal packing and contains two triple-helical molecules unlike the structure of (Hyp^R-Hyp^R-Gly)$_{10}$ shown in Figure 4a. At the level of molecular conformation, there are some differences as well in ϕ and ψ angles of Hyp^R at the X and Y positions. The comparisons of averaged values of backbone dihedral angles ϕ, ψ, and ω demonstrated that the absolute values of ϕ and ψ of Hyp^R at the X and Y positions of (Gly-Hyp^R-Hyp^R)$_9$ are appreciably larger than those of (Hyp^R-Hyp^R-Gly)$_{10}$ (see Table S2 in the Supporting Information). These structural distinctions might result from the differences of the crystallization conditions such as a peptide concentration, pH, and precipitating agent. Although it is not clear whether these conformational differences are retained in solution state, they speculated the polyproline II conformation might be retained in (Gly-Hyp^R-Hyp^R)$_9$ at its single-stranded state because they observed CD spectra indicating the existence of such a secondary structure for Ac-(Gly-Hyp^R-Hyp^R)$_{10}$-NH$_2$ at 95 °C. Unfortunately, the CD spectra of (Gly-Hyp^R-Hyp^R)$_9$ itself have not been reported so far. If their speculation is correct, this could be the most distinguished difference of structural property between our (Hyp^R-Hyp^R-Gly)$_{10}$ and their (Gly-Hyp^R-Hyp^R)$_9$. Obviously, in the CD spectra of (Hyp^R-Hyp^R-Gly)$_{10}$, any ordered structure was not detected at higher temperature.

The Factor Stabilizing the Triple-Helical Structure for (Hyp^R-Hyp^R-Gly)$_{10}$. In the crystal structure of (Hyp^R-Hyp^R-Gly)$_{10}$, the majority of water molecules could be located with the precision that allowed us to identify peptide−solvent interactions. Because, at some parts of the triple helix of both peptides, water bridges are missing, the positions of water molecules forming the bridges are superimposed to demonstrate the preferential hydration pattern in Figure 8. Comparing the crystallographic data of (Hyp^R-Hyp^R-Gly)$_{10}$ and Gly → Ala with respect to the spatial distribution of water molecules, it is obvious that the difference of the distribution of water molecules is localized surrounding Hyp^R(X) OH of (Hyp^R-Hyp^R-Gly)$_{10}$. The ranges where waters distribute are classified into 10 areas as in Figure 8. They are located in almost the same manner except for areas 2 and 3. The typical profile of networks of water bridges observed in (Hyp^R-Hyp^R-Gly)$_{10}$ is demonstrated using water molecules such as W1, W2, ... picked up from areas 1, 2, ..., respectively, along with that of Gly → Ala in Figure 8. Three networks are commonly observed in the both peptides. They are (1) the intrachain network connecting Gly C═O and Hyp^R(Y) OH through W9 and W10, (2) the other intrachain network connecting Hyp^R(Y) C═O and Gly C═O through W5 and W7 (occasionally via W6), and (3) the interchain network connecting Hyp^R(Y) OH and Hyp^R-(Y) C═O in the adjacent chain through W8 and W4. [Water bridges in each case are named γ for (1), α for (2), and δ for (3), respectively.]

In Gly→ Ala, which is devoid of the hydroxyl group at the X position, there is a long interchain water bridge composed of four waters, W1, W2, W3, and W4, which connect Gly C═O and Hyp^R(Y) C═O in the adjacent chain. (This is named the β water bridge.) On the contrary, there are two water bridges in (Hyp^R-Hyp^R-Gly)$_{10}$ different from the one observed in Gly → Ala. One of them is an interchain water bridge composed of W1 and W3 (occasionally via W2) which connects Gly C═O and Hyp^R(X) OH in the adjacent chain, and the other is an intrachain water bridge composed of W4 which connects Hyp^R(X) OH and Hyp^R(Y) C═O. (These two are named κ and λ water bridges, respectively, and furthermore, the water bridge composed of W4 and W8 connecting Hyp^R(X) OH and Hyp^R(Y) OH is named μ.) Consequently, the interchain interaction between Gly C═O and Hyp^R(Y) C═O is strengthened by fixing the two water bridges, κ and λ, on the pivot of Hyp^R(X) OH in (Hyp^R-Hyp^R-Gly)$_{10}$, whereas the water bridge β connects them via an intervening water molecule in Gly → Ala. The presence of these two water bridges results from the conformation of the hydroxyl group of the Hyp^R residue taking the up pucker. Therefore, this up pucker is considered as the favorable conformation of Hyp^R in (Hyp^R-Hyp^R-Gly)$_{10}$ at the X

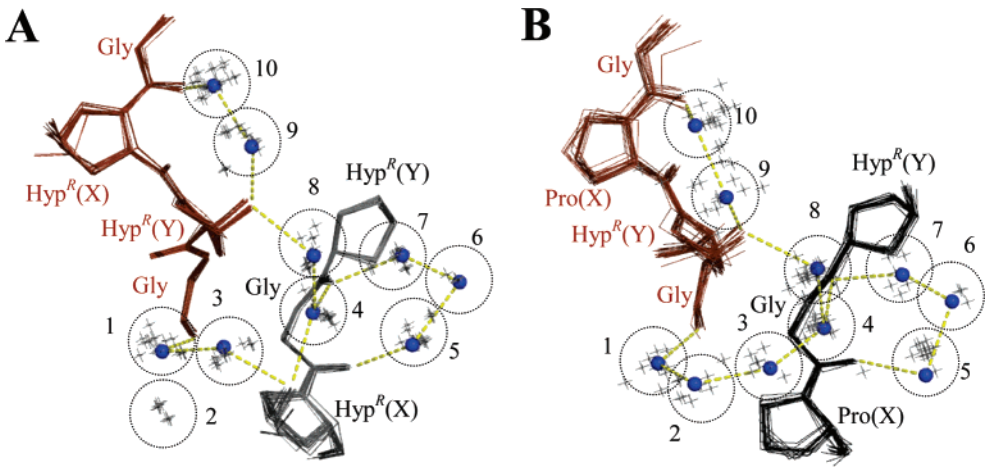

FIGURE 8: Distribution of water molecules which participate in the water bridge observed in (Hyp^R-Hyp^R-Gly)$_{10}$ (A) and Gly → Ala (B). (A) The triple-helical structure of (Hyp^R-Hyp^R-Gly)$_{10}$ is projected on its cross section. The two peptide segments, Gly-Hyp^R(X)-Hyp^R(Y)-Gly and Hyp^R(Y)-Gly-Hyp^R(X), which interact with each other to form the triple helix, are illustrated by superposition of 30 peptide units with the positions of waters involved in the water bridge network. (B) The two peptide fragments, Gly-Pro(X)-Hyp^R(Y)-Gly and Hyp^R-(Y)-Gly-Pro(X), of Gly → Ala are illustrated by superposition of 21 peptide units. The peptide fragments including Ala residues are omitted. An example of a water molecule which participates in the network is colored in blue. Dotted lines (yellow) designate the hydrogen bonds.

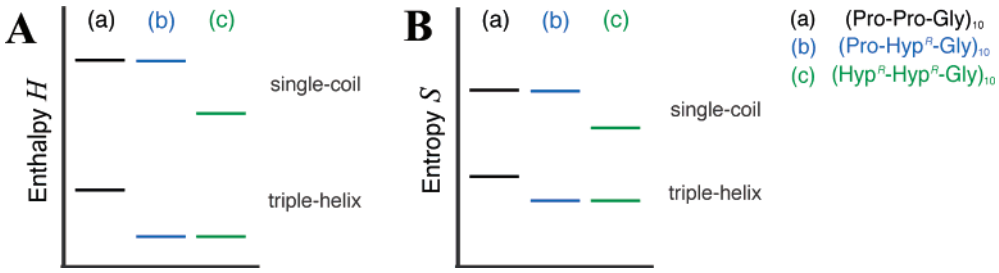

FIGURE 9: Enthalpy (A) and entropy (B) diagrams in triple-helix and single-coil states for (a) (Pro-Pro-Gly)$_{10}$, (b) (Pro-Hyp^R-Gly)$_{10}$, and (c) (Hyp^R-Hyp^R-Gly)$_{10}$.

position. The exceptional down pucker found in the three Hyp^R residues, A10, B16, and C25 (all at the X position), could be the consequence of a strong structural requirement for the packing of the triple helices in the crystal structure (Figure 4a).

As mentioned above, in the crystals of (Hyp^R-Hyp^R-Gly)$_{10}$, we recognized that the addition of water bridges κ, μ, and λ to water bridges of α, β, γ, and δ found in Gly → Ala (*10*) might imply an increase in the number of water molecules involved in the hydration. However, the existence of the water molecules participating simultaneously in two or three water bridges seems to make this implication invalid. As shown in Figure 8, the W4 is involved simultaneously in three kinds of water bridges, δ, λ, and μ, and W8 is involved in μ and δ water bridges.

On the basis of these crystallographic data, we correlate, as reported in our recent study (*13*), the location and number of water molecules with the effect of hydration which is deduced from the measurement of partial specific volume and the calculations of molecular volume and ASA. Comparing the hydration volumes ($V_{hyd,t}$) listed in Table 6, we note that the value of -19.0 cm^3 mol^{-1} determined for (Hyp^R-Hyp^R-Gly)$_{10}$ is about twice that of -9.6 cm^3 mol^{-1} for (Pro-Pro-Gly)$_{10}$ and is very close to -18.6 cm^3 mol^{-1} for (Pro-Hyp^R-Gly)$_{10}$ (*13*). From these data, we can assume that the triple helices of (Hyp^R-Hyp^R-Gly)$_{10}$ and (Pro-Hyp^R-Gly)$_{10}$ are hydrated with about the same number of water molecules, whereas the additional hydroxyl group of Hyp^R in (Hyp^R-Hyp^R-Gly)$_{10}$ is available for further hydration. Therefore, the increase in the number of types of water bridges does not necessarily lead to the increase in the number of hydrated waters.

It has been shown in the previous paper that comparing to (Hyp^R-Hyp^R-Gly)$_{10}$ and (Pro-Hyp^R-Gly)$_{10}$, both ΔH and ΔS of the former are obviously smaller than those of the latter (*26*). This is incompatible with the fact that there is no significant difference in degrees of hydration between them in the triple-helix state. Thus, we wonder if the additional Hyp^R residues cause the additional hydration on the peptides in their single-stranded state. If so, we would be able to explain the characteristic thermodynamic parameters where the enthalpy and entropy changes of (Hyp^R-Hyp^R-Gly)$_{10}$ are notably smaller than those of (Pro-Hyp^R-Gly)$_{10}$ (*26*).

The $V_{hyd,s}$ values for (Pro-Pro-Gly)$_{10}$, (Pro-Hyp^R-Gly)$_{10}$, and (Hyp^R-Hyp^R-Gly)$_{10}$ were determined to be -2.6, -4.0, and -7.3 cm^3 mol^{-1}, respectively, as listed in Table 6, indicating that the degrees of hydration of (Pro-Pro-Gly)$_{10}$ and (Pro-Hyp^R-Gly)$_{10}$ in the single-coil state are almost the same whereas that of (Hyp^R-Hyp^R-Gly)$_{10}$ is obviously larger.

Taking account of the fact that hydration contributes to decrease enthalpy, we concluded that the enthalpy of (Hyp^R-Hyp^R-Gly)$_{10}$ in the triple-helix state does not differ from that of (Pro-Hyp^R-Gly)$_{10}$ and is smaller than that of (Pro-Pro-Gly)$_{10}$. On the other hand, the enthalpy of (Hyp^R-Hyp^R-Gly)$_{10}$ in the single-coil state is smaller than those of (Pro-Pro-

Gly)$_{10}$ and (Pro-Hyp^R-Gly)$_{10}$, which are similar. To summarize, an enthalpy diagram for these model peptides is shown in Figure 9A.

In the discussion of the thermal stability of triple-helical structure, enthalpy is often overemphasized. As the Gibbs free energy change (ΔG) associated with the transition from the triple-helix to single-coil composes enthalpy (ΔH) and entropy (ΔS) changes, the comparison of ΔS as well as ΔH among these three model peptides is indispensable for clarifying the stabilizing mechanism of (Hyp^R-Hyp^R-Gly)$_{10}$. Hydration reduces the entropy because of the restriction of motional freedom of the water molecules surrounding the peptide molecule. Therefore, the entropy of (Hyp^R-Hyp^R-Gly)$_{10}$ in the triple-helix state does not significantly differ from that of (Pro-Hyp^R-Gly)$_{10}$ and is smaller than that of (Pro-Pro-Gly)$_{10}$. On the other hand, CD measurements showed that neither of these model peptides in the single-coil state seems to take any ordered secondary structure like polyproline II (Figure 6A; also Figures 3A,B in ref *13*). This suggests that the conformational entropies of these model peptides in the single-coil state are essentially the same.[2] From volumetric experiments, the hydration entropy of (Hyp^R-Hyp^R-Gly)$_{10}$ in the single-coil state is smaller than those of (Pro-Pro-Gly)$_{10}$ and (Pro-Hyp^R-Gly)$_{10}$, which are considered to be almost the same. Therefore, the total entropy of (Hyp^R-Hyp^R-Gly)$_{10}$ in the single-coil state is smaller than those of (Pro-Pro-Gly)$_{10}$ and (Pro-Hyp^R-Gly)$_{10}$. The smaller ΔH and ΔS of (Hyp^R-Hyp^R-Gly)$_{10}$ than those of (Pro-Pro-Gly)$_{10}$ and (Pro-Hyp^R-Gly)$_{10}$ are ascribed to the high degree of hydration of (Hyp^R-Hyp^R-Gly)$_{10}$ in the single-coil state. An entropy diagram is given in Figure 9B as well.

CONCLUSION

As the main factor that stabilizes its triple-helical structure, we deduced that a high degree of hydration of (Hyp^R-Hyp^R-Gly)$_{10}$ in the single-coil state plays a key role in the thermal stability of this peptide. The hydroxyl group of Hyp^R at the X position of (Hyp^R-Hyp^R-Gly)$_{10}$ allows the additional hydration in the single-coil state, resulting in a smaller enthalpy change than those of (Pro-Hyp^R-Gly)$_{10}$ and (Pro-Pro-Gly)$_{10}$. The smaller entropy change of (Hyp^R-Hyp^R-Gly)$_{10}$ is, in contrast, caused more significantly by the possible extensive hydration that restricts the mobility of water molecules. This demonstrates that investigation of the collagen model peptide in the single-coil state as well as in the triple-helix state is crucial in obtaining a comprehensive explanation for the stabilizing mechanism of the collagen triple helix.

ACKNOWLEDGMENT

We thank Dr. Shigeru Kubo (Peptide Institute Inc.) for the characterization of the model peptides with mass spectrometry and Ms. Yoshiko Yagi (Institute for Protein Research, Osaka University) for the precise amino acid analyses for concentration determination of peptide solution. We also thank Dr. Evelyn R. Stimson for helpful discussion.

SUPPORTING INFORMATION AVAILABLE

Calculation of the degree of hydration of the single-coil state of (Pro-Pro-Gly)$_{10}$, (Pro-Hyp^R-Gly)$_{10}$, and (Hyp^R-Hyp^R-Gly)$_{10}$, concentration dependencies of the density of the apparent molecular weights of (Hyp^R-Hyp^R-Gly)$_{10}$, comparison of the Rich and Crick II hydrogen bond patterns by molecular modeling, and averaged values of main- and side-chain dihedral angles of the model peptides. This material is available free of charge via the Internet at http://pubs.acs.org.

REFERENCES

1. Baum, J., and Brodsky, B. (2000) Folding of the collagen triple-helix and its naturally occurring mutants, in *Mechanisms of Protein Folding* (Pain, R. H., Ed.) 2nd ed., pp 330−351, Oxford University Press, Oxford, U.K.
2. Ramachandran, G. N., and Kartha, G. (1955) Structure of collagen, *Nature 176*, 593−595.
3. Rich, A., and Crick, F. H. C. (1961) The molecular structure of collagen, *J. Mol. Biol. 3*, 483−506.
4. Sakakibara, S., Kishida, Y., Kikuchi, Y., Sakai, R., and Kakiuchi, K. (1968) Synthesis of poly-(L-prolyl-L-prolylglycyl) of defined molecular weights, *Bull. Chem. Soc. Jpn. 41*, 1273.
5. Kobayashi, Y., Sakai, R., Kakiuchi, K., and Isemura, T. (1970) Physicochemical analysis of (Pro-Pro-Gly)$_n$ with defined molecular weight-temperature dependence of molecular weight in aqueous solution, *Biopolymers 9*, 415−425.
6. Sakakibara, S., Inouye, K., Shudo, K., Kishida, Y., Kobayashi, Y., and Prockop, D. J. (1973) Synthesis of (Pro-Hyp-Gly)$_n$ of defined molecular weights. Evidence for the stabilization of collagen triple helix by hydroxyproline, *Biochim. Biophys. Acta 303*, 198−202.
7. Uchiyama, S., Kai, T., Kajiyama, K., Kobayashi, Y., and Tomiyama, T. (1997) Measurement of thermodynamic quantities in the heating-rate dependent thermal transitions of sequenced polytripeptides, *Chem. Phys. Lett. 281*, 92−96.
8. Nishi, Y., Doi, M., Uchiyama, S., Nishiuchi, Y., Nakazawa, T., Ohkubo, T., and Kobayashi, Y. (2003) Stabilization mechanism of triple helical structure of collagen molecules, *Lett. Pept. Sci. 10*, 533−537.
9. Bella, J., Eaton, M., Brodsky, B., and Berman, H. M. (1994) Crystal and molecular structure of a collagen-like peptide at 1.9 Å resolution, *Science 266*, 75−81.
10. Bella, J., Brodsky, B., and Berman, H. M. (1995) Hydration structure of a collagen peptide, *Structure 3*, 893−906.
11. Holmgren, S. K., Taylor, K. M., Bretscher, L. E., and Raines, R. T. (1998) Code for collagen's stability deciphered, *Nature 392*, 666−667.
12. Holmgren, S. K., Bretscher, L. E., Taylor, K. M., and Raines, R. T. (1999) A hyper stable collagen mimic, *Chem. Biol. 6*, 63−70.
13. Nishi, Y., Uchiyama, S., Doi, M., Nishiuchi, Y., Nakazawa, T., Ohkubo, T., and Kobayashi, Y. (2005) Different effects of 4-hydroxyproline and 4-fluoroproline on the stability of collagen triple helix, *Biochemistry 44*, 6034−6042.
14. Inouye, K., Sakakibara, S., and Prockop, D. J. (1976) Effects of the stereo-configuration of the hydroxyl group of in 4-hydroxyproline on the triple-helical structures formed by homogeneous peptides resembling collagen, *Biochim. Biophys. Acta 420*, 133−141.

[2] As mentioned above, Bächinger and co-workers claimed that (Gly-Hyp^R-Hyp^R)$_9$ takes the polyproline II conformation even in the single-coil state (*27*). They also speculated that such a conformation is stabilized by an intrastranded water-mediated bridge which corresponds to the λ water bridge even at higher temperature. If these speculations are correct, the mechanism of the stability of (Gly-Hyp^R-Hyp^R)$_9$ should be quite different from our case of (Hyp^R-Hyp^R-Gly)$_{10}$. For example, ΔS between three-stranded and single-stranded states in the case of (Gly-Hyp^R-Hyp^R)$_9$ would be exceptionally small. However, we would like to raise questions whether they took the difference of thermal stabilities between Ac-(Gly-Hyp^R-Hyp^R)$_{10}$-NH$_2$ and (Gly-Hyp^R-Hyp^R)$_9$ into account and whether the system of their Ac-(Gly-Hyp^R-Hyp^R)$_{10}$-NH$_2$ had completely reached the single-stranded state after the transition. Owing to the use of an airtight pressure-proof cell compartment (*35*, *36*), we could measure the melting curve of (Hyp^R-Hyp^R-Gly)$_{10}$ at a temperature range which is wide enough to ensure the completion of the transition to obtain ΔH and ΔS correctly.

15. Inouye, K., Kobayashi, Y., Kyogoku, Y., Kishida, Y., Sakakibara, S., and Prockop, D. J. (1982) Synthesis and physical properties of (hydroxyproline-proline-glycine)$_{10}$: Hydroxyproline in the X-position decreases the melting temperature of the collagen triple helix, *Arch. Biochem. Biophys. 219*, 198−203.
16. Vitagliano, L., Berisio, R., Mazzarella, L., and Zagari, A. (2001) Structural bases of collagen stabilization induced by proline hydroxylation, *Biopolymers 58*, 459−464.
17. Vitagliano, L., Berisio, R., Mastrangelo, A., Mazzarella, L., and Zagari, A. (2001) Preferred proline puckerings in *cis* and *trans* peptide groups: implications for collagen stability, *Protein Sci. 10*, 2627−2632.
18. Doi, M., Nishi, Y., Kiritoshi, N., Iwata, T., Nago, M., Nakano, H., Uchiyama, S., Nakazawa, T., Wakamiya, T., and Kobayashi, Y. (2002) Simple and efficient synthesis of Boc- and Fmoc-protected 4(*R*)- and 4(*S*)-fluoroproline solely from 4(*R*)-hydroxyproline, *Tetrahedron 58*, 8453−8459.
19. Gerig, J. T., and McLeod, R. S. (1973) Conformations of *cis*- and *trans*-4-fluoro-L-proline in aqueous solution, *J. Am. Chem. Soc. 95*, 5725−5729.
20. Shamala, M., Row, T. N. G., and Venkatesan, K. (1976) Crystal and molecular structure of allo-4-hydroxy-L-proline dehydrate, *Acta Crystallogr., Sect. B 32*, 3267−3270.
21. Panasik, N., Jr., Eberhardt, E. S., Edison, A. S., Powell, D. R., and Raines, R. T. (1994) Inductive effects on the structure of proline residues, *Int. J. Pept. Protein Res. 44*, 262−269.
22. Improta, R., Benzi, C., and Barone, V. (2001) Understanding the role of stereoelectronic effects in determining collagen stability. 1. A quantum mechanical study of proline, hydroxyproline, and fluoroproline dipeptide analogues in aqueous solution, *J. Am. Chem. Soc. 123*, 12568−12577.
23. DeRider, M. L., Wilkens, S. T., Waddell, M. J., Bretscher, L. E., Weinhold, F., Raines, R. T., and Markley, J. L. (2002) Collagen stability: insights from NMR spectroscopic and hybrid density functional computational investigations of the effect of electronegative substituents on prolyl ring conformations, *J. Am. Chem. Soc. 124*, 2497−2505.
24. Mizuno, K., Hayashi, T., Peyton, D. H., and Bächinger, H. P. (2004) Hydroxylation-induced stabilization of the collagen triple helix. Acetyl-(glycyl-4(*R*)-hydroxyprolyl-4(*R*)-hydroxyprolyl)$_{10}$-NH_2 forms a highly stable triple helix, *J. Biol. Chem. 279*, 38072−38078.
25. Berisio, R., Granata, V., Vitagliano, L., and Zagari, A. (2004) Imino acids and collagen triple helix stability: characterization of collagen-like polypeptides containing Hyp-Hyp-Gly sequence repeats, *J. Am. Chem. Soc. 126*, 11402−11403.
26. Doi, M., Nishi, Y., Uchiyama, S., Nishiuchi, Y., Nishio, H., Nakazawa, T., Ohkubo, T., and Kobayashi, Y. (2005) Collagen-like triple helix formation of synthetic (Pro-Pro-Gly)$_{10}$ analogues: (4(*S*)-hydroxyprolyl-4(*R*)-hydroxyprolyl-Gly)$_{10}$, (4(*R*)-hydroxyprolyl-4(*R*)-hydroxyprolyl-Gly)$_{10}$ and (4(*S*)-fluoroprolyl-4(*R*)-fluoroprolyl-Gly)$_{10}$, *J. Pept. Sci. 11*, 609−616.
27. Schumacher, M., Mizuno, K., and Bächinger, H. P. (2005) The crystal structure of the collagen-like polypeptide (glycyl-4(*R*)-hydroxyprolyl-4(*R*)-hydroxyprolyl)$_9$ at 1.55 Å resolution shows up-puckering of the proline ring in the Xaa position, *J. Biol. Chem. 280*, 20397−20403.
28. Pflugrath, J. W. (1999) The finer things in X-ray diffraction data collection, *Acta Crystallogr., Sect. D 55*, 1718−1725.
29. Mattews, B. W. (1968) Solvent content of protein crystals, *J. Mol. Biol. 33*, 491−497.
30. Foadi, J., Woolfson, M. M., Dodson, E. J., Wilson, K. S., Jiaxing, Y., and Chao-de, Z. (2000) A flexible and efficient procedure for the solution and phase refinement of protein structures, *Acta Crysallogr., Sect. D 56*, 1137−1147.
31. Berisio, R., Vitagliano, L., Mazzarella, L., and Zagari, A. (2002) Crystal structure of the collagen triple helix model [(Pro-Pro-Gly)$_{10}$]$_3$, *Protein Sci. 11*, 262−270.
32. Perrakis, A., Morris, R., and Lamzin, V. S. (1999) Automated protein model building combined with iterative structure refinement, *Nat. Struct. Biol. 6*, 458−463.
33. McRee, D. E. (1999) XtalView/Xfit−A versatile program for manipulating atomic coordinates and electron density, *J. Struct. Biol. 125*, 156−165.
34. Murshudov, G. N., Vagin, A. A., Lebedev, A., Wilson, K. S., and Dodson, E. J. (1999) Efficient anisotropic refinement of macromolecular structures using FFT, *Acta Crystallogr., Sect. D 55*, 247−255.
35. Uchiyama, S., Ohshima, A., Nakamura, S., Hasegawa, J., Terui, N., Takayama, S. J., Yamamoto, Y., Sambongi, Y., and Kobayashi, Y. (2004) Complete thermal-unfolding profiles of oxidized and reduced cytochromes *c*, *J. Am. Chem. Soc. 126*, 14684−14685.
36. Ohshima, A., Uchiyama, S., Nakano, H., Yoshida, T., Ohkubo, T., and Kobayashi, Y. (2003) CD measurement of aqueous protein solution at high temperature up to 180 °C−Thermodynamic analysis of thermophilic protein by pressure-proof cell compartment, *Lett. Pept. Sci. 10*, 539−543.
37. Kupke, D. W. (1973) Density and volume change measurements, in *Physical Principles and Techniques of Protein Chemistry* (Leach, S. J., Ed.) Part C, pp 1−75, Academic Press, New York.
38. Brünger, A. T. (1992) *X-PLOR Version 3.1: A System for X-ray Crystallography and NMR*, Yale University, New Haven, CT.
39. Connolly, M. L. (1983) Analytical molecular surface calculation, *J. Appl. Crystallogr. 16*, 548−558.
40. Okuyama, K., Arnott, S., Takayanagi, M., and Kakudo, M. (1981) Crystal and molecular structure of a collagen-like polypeptide (Pro-Pro-Gly)$_{10}$, *J. Mol. Biol. 152*, 427−443.
41. Kramer, R. Z., Vitagliano, L., Bella, J., Berisio, R., Mazzarella, L., Brodsky, B., Zagari, A., and Berman, H. M. (1998) X-ray crystallographic determination of a collagen-like peptide with the repeating sequence (Pro-Pro-Gly), *J. Mol. Biol. 280*, 623−638.
42. Nagarajan, V., Kamitori, S., and Okuyama, K. (1998) Crystal structure analysis of collagen model peptide (Pro-Pro-Gly)$_{10}$, *J. Biochem. 124*, 1117−1123.
43. Nagarajan, V., Kamitori, S., and Okuyama, K. (1999) Structure analysis of a collagen-model peptide with a (Pro-Hyp-Gly) sequence repeat, *J. Biochem. 125*, 310−318.
44. Kramer, R. Z., Venugopal, M. G., Bella, J., Mayville, P., Brodsky, B., and Berman, H. M. (2000) Staggered molecular packing in crystals of a collagen-like peptide with a single charged pair, *J. Mol. Biol. 301*, 1191−1205.
45. Berisio, R., Vitagliano, L., Mazzarella, L., and Zagari, A. (2001) Crystal structure of a collagen-like polypeptide with repeating sequence Pro-Hyp-Gly at 1.4 Å resolution: implications for collagen hydration, *Biopolymers 56*, 8−13.
46. Delano, W. L. (2001) *PyMOL*, DeLano Scientific, LLC, San Carlos, CA.

BI051619M